

## Specific heat relaxation during macromolecule growth

C. Ferrari, G. Salvetti, and E. Tombari

*Istituto di Fisica Atomica e Molecolare del Consiglio Nazionale delle Ricerche, Via del Giardino 7, 56100 Pisa, Italy*

G. P. Johari

*Department of Materials Science and Engineering, McMaster University, Hamilton, Ontario, Canada L8S-4L7*

(Received 7 December 1995)

When dissimilar molecules in a liquid mixture react isothermally to form covalent bonds and linear chain macromolecules grow until the liquid vitrifies, the complex  $C_p$  of the mixture measured for a fixed frequency decreases. The real component of this  $C_p$  measured as a function of the number of covalent bonds formed, or macroscopic reaction time, shows a dispersionlike decrease and the imaginary component a peak. From these data, the evolution of structural relaxation time during the growth of the macromolecules has been determined and its formalism given. [S1063-651X(96)50908-6]

PACS number(s): 61.25.Hq, 64.70.Pf, 82.60.Fa

When molecules in a liquid spontaneously combine to produce a covalently bonded structure, the size of the diffusing entity grows continuously and irreversibly at a fixed temperature. This alters the molecular dynamics of the liquid as its density, viscosity, and molecular diffusion, or relaxation time, all increase when van der Waal's and other weak interactions are replaced by covalent bonds and the number of configurational states available to the structure of the liquid decreases irreversibly under isothermal conditions. Increase in the molecular diffusion time on the growth of a macromolecule in turn slows the rate of the very chemical reaction that allows the macromolecule's growth [1]. Thus a so-called negative feedback between the physical and chemical processes reduces the rate of both diffusion and reaction such that, when a certain number of covalent bonds has formed, chemical and physical changes become unobservable over a period of  $\sim 10^3$  s and the liquid is said to have vitrified under isothermal conditions. This is accompanied by a freezing-in of molecular dynamics of the liquid, which in turn is reflected in the measured thermodynamic functions. By using a technique developed for studying this phenomenon, we have measured simultaneously the heat evolved during this process and the real and imaginary components of heat capacity  $C_p$ , i.e.,  $C_p'$  and  $C_p''$ , without the complications arising from the dynamic thermal conductivity. Here we report a study of the growth of a linear chain macromolecule formed by reaction between *n*-hexylamine (molecule *A*) and diglycidyl ether of bisphenol-*A* (molecule *B*) in molar ratio of 1:1. It should be stressed that the observation of this phenomenon is important here; the choice of material is incidental.

A microcalorimeter with a differential cell configuration was used for determining  $\Delta H$ , the heat evolved during the course of chemical reactions that led to the macromolecule's growth, and  $C_p$  of the liquid during this growth. It consisted of two identical cells containing mercury, each constructed from a closed-end stainless steel tube, 100 mm long, 4.7 mm internal diameter and 0.15 mm wall thickness. It was wound on its outside with a heater wire and thereafter a sensor. Each as a whole was kept inside a thermal bath with  $H_2$  gas at 1 bar, which served as a heat transmitting medium between the isothermal bath and the cell, as shown in Fig. 2 of Ref. [2].

Two identical Pyrex glass tubes of 80 mm length, 2.2 mm internal diameter, and 0.25 mm wall thickness were immersed one each in the mercury contained in each cell. The glass tube immersed in one cell contained the liquid sample and that immersed in the second, identical cell acting as a reference, was kept empty. Immersion of the tubes in mercury ensured excellent thermal contact between the sample, heater, and the sensor. The cell was heated by a sinusoidal power signal,  $P(t')$  of known amplitude and frequency, superimposed on a constant value  $P_0$ , such that  $P(t') = P_0[1 + \cos(\omega t')]$ , where  $\omega$  is the angular frequency and  $t'$  the time. The dissipation of this power occurred in two ways, (a) through the cell walls to the thermal bath, and (b) through the cell walls to the mercury, the Pyrex tube and the sample, all arranged concentrically.  $C_p'$  and  $C_p''$  were determined from the changes in the amplitude and the phase angle of the observed sinusoidal temperature profile. The microcalorimeter was calibrated by an independent procedure using a sinusoidal heat pulse.

Within the approximation of linear response, the calorimetric cell can be described as an electrical circuit with distributed loss and storage components [3]. In this manner, the complex temperature  $T_x^*$  of the cell sensor is related to the complex equivalent electrical admittance  $Y^*$  by  $T_x^* - T_0^* = A^* Y^* / (1 + B^* Y^*)$  where  $T_0^*$  is the complex temperature of the cell without the sample and  $A^*$  and  $B^*$  are the instrument's constants which are frequency- and temperature-dependent, according to our deduction from Eq. (2.24) in Ref. [3].

In this assembly, the sample was heated from the surrounding, and so the equations for the heat flow are analogous to those in the case [3] when the sample is heated from its core. From the dimensions of our sample and from these equations, we used  $Y^* = i\omega C_p^*$ . For the frequency,  $10^{-2}$  Hz, used here, this approximation causes at most 2% error in our  $C_p$  values.

As the heat was released during the macromolecule's growth, the sample cell's temperature increased in proportion to the rate of heat release. The effect of the sinusoidal power input of frequency  $\omega$  was superposed on this temperature-time profile. The numerical average of the tem-

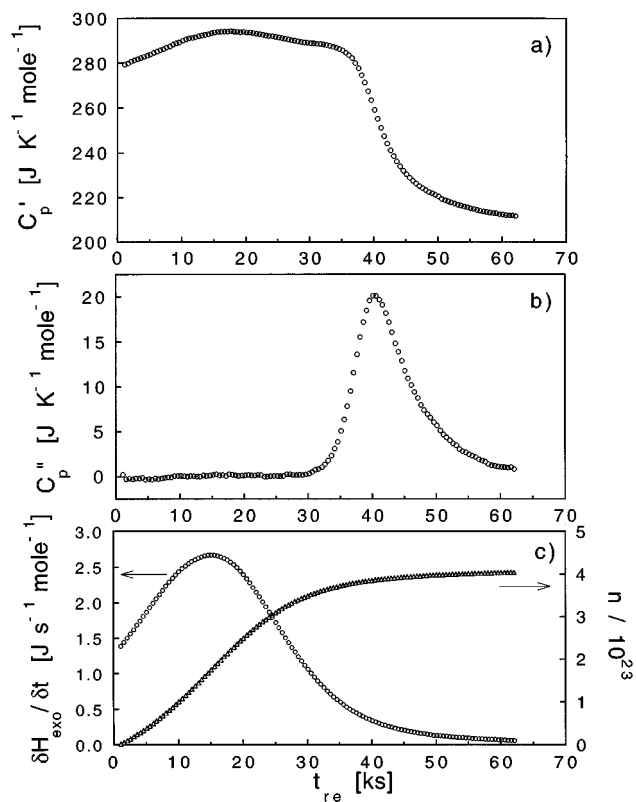


FIG. 1. The (a) real and (b) imaginary components of specific heat at 0.01 Hz measured during the linear chain growth, i.e.,  $-A-B-A-B-$  structure, with  $A$  being  $n$ -hexylamine and  $B$ , diglycidyl ether of bisphenol  $A$  at 300.1 K. In this process, the nitrogen atom of  $n$ -hexylamine covalently bonds with one terminal carbon atom of the epoxy groups of two  $B$  molecules. Part (c) contains a plot of the heat release  $(\partial H/\partial t)_T$  and a plot of the number of covalent bonds formed as the reaction occurred. The plots are against time during the course of the macromolecule's growth.

perature over one cycle, after calibration with a known power from a heater, provided the value of  $\partial H/\partial t$ , simultaneously with  $C_p'$  and  $C_p''$ .

Figures 1(a)–1(c) show direct measurements of  $C_p'$ ,  $C_p''$  and the heat evolved during the course of the macromolecule's growth at 300.1 K. The total heat evolved,  $\Delta H_{\text{total}}$ , is the area under the curve labeled  $(\partial H/\partial t)_T$  shown in Fig. 1(c), and would be equal to the total heat evolved when integration is done up to  $t$  approaching infinity, when polymerization will be complete. But since measurements were done only up to 63 ks, during which time polymerization did not reach completion, this area gives only a fraction of the heat evolved during the macromolecule's growth. So a further experiment was done in which the sample was rate-heated and the rest of the heat evolved during polymerization determined by integration of a curve obtained on a temperature ramp. The total heat evolved,  $\Delta H_{\text{total}}$ , is the sum of the heat evolved isothermally as determined from the area under the curve in Fig. 1(c) and the heat evolved during the rate-heating in the further experiment. This heat is directly proportional to the number of covalent bonds formed and since the total number of such bonds formed is equal to the Avogadro number ( $6.03 \times 10^{23}$ ), and the bonding between 0.5 moles of  $A$  and 0.5 moles of  $B$  leads to the  $A-B-A-B-$

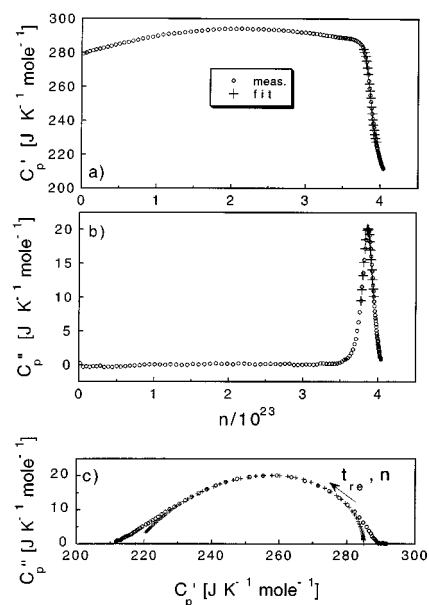


FIG. 2. The plots of (a)  $C_p'$  and (b)  $C_p''$  against  $n$  and (c) the complex plane plots of  $C_p''$  and  $C_p'$  at 0.01 Hz. Crosses represent the data points calculated from Eqs. (5), (6), and (2) with  $\gamma=0.55$ . In (c) the number of bonds formed increases from right to left. The process is irreversible.

chain structure, the total number of bonds formed at time  $t$  is given by  $n(t) = 6.03 \times 10^{23} [\Delta H(t)/\Delta H_{\text{total}}]$ . But, because of the prohibitive slowness of the chemical reactions,  $\Delta H$  measured under isothermal conditions at 300.1 K is much less than  $\Delta H_{\text{total}}$ , and so the number of bonds formed did not reach  $6.03 \times 10^{23}$  after reactions had occurred for 23 ks at 300.1 K. Thus,  $n(t)$  calculated from  $\Delta H(t)$ , which has been plotted against the time of reaction in Fig. 1(c), does not reach  $6.03 \times 10^{23}$ . Using this variation of  $n$  with  $t$ , the  $t$  dependence of  $C_p'$  and  $C_p''$  was converted to their  $n$  dependence for which the plot against  $n$  is shown in Fig. 2(a). The shape of these plots resembles the  $C_p'$  and  $C_p''$  spectra of liquids in the frequency domain where the structure and/or dynamics remains unchanged with time [4].

The low  $n$  limit of  $C_p'$  ( $=285 \text{ J mol}^{-1} \text{ K}^{-1}$ ) in Fig. 2(c) represents the specific heat of the liquid sample when the characteristic relaxation times of the internal modes are shorter than the experimental time window. This is the usual thermodynamic  $C_p$  measured when enough time is taken to allow all the "internal modes" to contribute. The high  $n$  limit of  $C_p'$  ( $=217.5 \text{ J mol}^{-1} \text{ K}^{-1}$ ) does not contain all contributions from those internal modes which fail to relax within the observation time.

To obtain information on the dynamic  $C_p$  response of the sample with increasing  $n$ , we consider first the molecular processes involved. Each one of the two types of molecules in the liquid forms two covalent bonds with the molecule of the other type, thus forming a chain sequence  $-A-B-A-B-$ . The ends of this chain may ultimately link together or not, depending upon the diffusion probability of the end molecules towards each other and the bond compatibility of the end molecules. This may lead to loop formation as well as to a distribution of chain lengths. When this irreversible growth occurs, or as  $n$  increases,  $C_p$  changes for at least five reasons: (i) a decrease in the concentration of

impurity ions as they associate to form ion pairs (this is also the origin of the observed dielectric permittivity decrease [1]), which alters the configurational contribution to  $C_p$ ; (ii) an increase in the molecular diffusion time which causes  $C_p'$  to decrease progressively from its molecular state ( $n=0$ ), to a macromolecular state ( $n \gg 0$ ), the lower value of  $C_p'$  representing the contribution from all the modes with characteristic frequency much lower than that used in the experiment; (iii) a change in the contribution to  $C_p$  from the high frequency modes as the vibrational frequencies increase and new vibrational modes with new density distribution become important; (iv) a change in the relaxation function as the liquid structure changes; and (v) a splitting of the unimodal relaxation function into a bimodal relaxation function corresponding to the  $\alpha$  and  $\beta$  processes [1,5]. Thus the complex  $C_p^*$  becomes  $n$  dependent, and in a general formalism:

$$\begin{aligned} C_p^*(\omega, n) &= C_p'(\omega, n) - iC_p''(\omega, n) \\ &= C_{p,\infty}(n) + [C_{p,0}(n) - C_{p,\infty}(n)] \\ &\quad \times \int_0^\infty -e^{-i\omega t} [\partial \phi(t) / \partial t]_n dt \end{aligned} \quad (1)$$

where  $C_{p,\infty}(n)$  and  $C_{p,0}(n)$  are the high and low frequency limits of the heat capacity, respectively, when  $n$  is fixed. For a molecular process,  $\phi(t)$  is generally defined as

$$[\phi(t)]_n = \exp\{-[t/\tau(n)]^{\beta(n)}\} \quad (2)$$

where  $\tau$  is the characteristic relaxation time,  $\beta$  an empirical parameter whose magnitude determines the shape of the spectra (when  $\beta=1$ , the spectrum is symmetrical and of the Debye form, and when  $0 < \beta < 1$  it is asymmetrically stretched from the Debye form) and  $t$  is the time for the observation of the perturbation's decay.

For a system whose state changes with time,  $n$  and  $\tau$ , strictly speaking, are time dependent and Eq. (2) is not applicable in strict terms. The period of the sinusoidal pulse we used was 100 s. In this case  $C_p'$  and  $C_p''$  may be measured accurately only when the rate of increase in  $n$  with  $t$  is insignificant during the sinusoidal signal period, or that the effect of such change is within the experimental errors.

Equation (1) for a structure-invariant system can be written as

$$C_p' = C_{p,\infty} + (C_{p,0} - C_{p,\infty})N' \quad (3)$$

and

$$C_p'' = (C_{p,0} - C_{p,\infty})N'' \quad (4)$$

by defining

$$N^*[\omega\tau(n), \beta(n)] = \int_0^\infty -e^{-i\omega t} [\partial \phi(t) / \partial t]_n dt \quad (5)$$

or

$$N' - iN'' = L(\partial \phi / \partial t)_n. \quad (6)$$

In the small range of  $n$  where the relaxation features in Fig. 2 appear, the terms  $[C_{p,0}(n) - C_{p,\infty}(n)]$  and  $\beta(n)$  can be as-

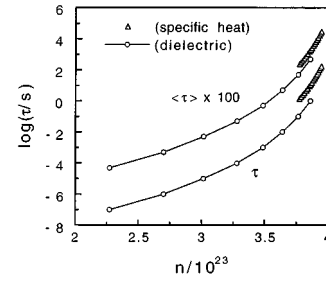


FIG. 3. The relaxation time calculated from the data in Figs. 1 and 2 is plotted against the number of bonds formed. Circles are the data from the corresponding dielectric measurements [7]. The lower plots are for the characteristic relaxation time  $\tau$  with  $\gamma=0.55$  [Eq. (3)]. The upper plots are for the average relaxation time. For clarity of plotting the data for the latter are multiplied by 100.

sumed to change with  $n$  negligibly in comparison with the many orders of increase in  $\tau$ , so that in a first approximation one obtains

$$C_p^*(\omega, n) = C_{p,\infty} + (C_{p,0} - C_{p,\infty})N^*(\omega\tau(n)). \quad (7)$$

Thus Eq. (7) becomes invariant of one's choice of  $\omega$  or  $\tau$ , and  $\beta(n)$  is replaced by a constant value,  $\gamma$ . In this manner each data point for a single frequency is described by  $\omega\tau(n)$ , and Kramers-Kronig relations are obeyed, but the entire curve (Fig. 2) is described by  $\gamma$  and  $\omega\tau$ . By analyzing the data of Fig. 2(c) according to Eq. (7),  $\gamma$  was found to be  $0.55 \pm 0.01$ . The characteristic relaxation time  $\tau$  was calculated for each point by determining the product  $\omega\tau$  for each measured value of  $C_p'(\omega\tau)$  and  $C_p''(\omega\tau)$  as described before for the dielectric data [1,5,6]. Since  $\omega$  is a constant this yields a value of  $\tau$  for each value of  $C_p^*$  measured for a certain  $n$  during the growth of the macromolecules. The resulting values of  $\tau$  are plotted against  $n$  in Fig. 3, where the corresponding data from the dielectric relaxation measurements [7], for which  $\gamma$  is 0.35, are included. The values of  $\tau$  from the  $C_p^*$  and dielectric measurements differ by nearly a factor of 10 where they are expected to overlap. Recognizing that the distribution of relaxation times differs for dielectric and structural relaxation, it is more appropriate to compare the average of the relaxation time,  $\langle \tau \rangle = (\pi/\gamma)\Gamma(1/\gamma)$ , where  $\Gamma$  represents the gamma function of  $(1/\gamma)$ . Within the experimental and analytical errors,  $\langle \tau \rangle$  from  $C_p^*$  seems to agree with that from dielectric measurements.

$C_p'$  and  $C_p''$  and their change with  $n$ , as measured here, for a fixed frequency can be discussed entirely in terms of the hydrodynamics of the liquid, i.e., in terms of isothermal changes in the viscosity and the bulk modulus, as discussed by Zwanzig [8]. In this consideration, the contributions from the hydrodynamic modes are lost more and more as the liquid becomes progressively more viscous isothermally with spontaneous increase in  $n$  or the chain length. The measured  $C_p$  appears to thus become  $n$  dependent because it is  $\tau$  in the product  $\omega\tau$ , and not  $\omega$ , that increases irreversibly and spontaneously with increase in  $n$ . This is the main difference between the  $C_p^*$  spectral [4], where  $\omega$  is deliberately varied at a constant temperature of a structurally invariant system, and the  $C_p^*$  variation studied here, where  $\tau$  increases spontaneously and irreversibly with  $t$  and  $n$ . When  $\tau$  becomes

longer in comparison with  $\omega^{-1}$  (the observation time as determined by  $\omega$ ), the internal or hydrodynamic modes of the newly formed structure in the liquid do not contribute fully to the entropy fluctuations of the liquid, and  $C_p$  acquires a real and an imaginary component. Thus the dynamic heat capacity is a direct consequence of the increase in  $n$  here through an increase in  $\tau$ . A peak in  $C_p''$  appears when  $\omega\tau=1$ . The decrease in  $C_p'$  with increase in  $n$ , as observed here, represents the change in the average entropy fluctuation according to the equation [9]

$$\Delta C_p = \frac{[(\overline{\Delta S^2})_{n=0} - (\overline{\Delta S^2})_{n=n(t)}]}{k_B} \quad (8)$$

where  $k_B$  is the Boltzmann constant.

We briefly consider why  $C_p'$  increased as  $n$  increased from its zero value during the beginning of the experiment [Fig. 1(a)]. Because there is no corresponding change in  $C_p''$ , this increase should result from an increase in the configurational and/or vibrational contributions with no corresponding

change in  $C_p''$ ; we attribute this increase to effect (i) described here earlier, namely to an increase in the number of accessible configurations when the dielectric permittivity decreases [5–7] with increase in  $n$ , and the impurity ions form ion pairs, thereby releasing dipolar parts of the molecule from their solvation shell.

In summary, from  $C_p$  relaxation of a time-variant system, we have shown how the relaxation time evolves during the irreversible growth of macromolecules and how the dynamics of this evolution differs from that observed in dielectric relaxation. Similar studies may be useful for examining also the dynamics of degradation of materials in which covalent bonds are broken by high-energy photon irradiation and where the relaxation time would decrease with decrease in  $n$ .

This research was supported partly by the Bilateral Research Agreement. G. P. J. is grateful for the hospitality and funds in support provided by IFAM del CNR, Pisa, during the period of his stay for this research. C. Ferrari is grateful to EDISON S.p.A. for a grant in support of this research.

- 
- [1] G. P. Johari, in *Disorder Effects in Relaxation Processes*, edited by R. Richert and A. Blumen (Springer Verlag, Berlin, 1994), p. 627.
- [2] M. Cassettari, F. Papucci, G. Salvetti, E. Tombari, S. Veronesi, and G. P. Johari, *Rev. Sci. Instrum.* **64**, 1076 (1993).
- [3] P. I. Somlo and J. D. Hunter, *Microwave Impedance Measurements*, IEE Electrical Measurements, Series 2 (Short Run Press Ltd. Exeter, 1985), p. 30.
- [4] N. O. Birge, *Phys. Rev. B* **34**, 1631 (1986).
- [5] E. Tombari and G. P. Johari, *J. Chem. Phys.* **97**, 6677 (1992).
- [6] M. G. Parthun and G. P. Johari, *J. Chem. Phys.* **103**, 440 (1995).
- [7] G. P. Johari and W. Pascheto, *J. Chem. Soc. Faraday Trans.* **91**, 343 (1995).
- [8] R. Zwanzig, *J. Chem. Phys.* **88**, 5831 (1988).
- [9] L. D. Landau and E. M. Lifshitz, *Statistical Physics* (Pergamon Press, Oxford, 1980).